Appl. Phys. B 70, 487–490 (2000) / Digital Object Identifier (DOI) 10.1007/s003409900180

Applied Physics B
Lasers
and Optics

Determination of the Auger upconversion rate in fiber-coupled diode end-pumped Nd:YAG and Nd:YVO_4 crystals

Y.F. Chen[1,*], **C.C. Liao**[2], **Y.P. Lan**[2], **S.C. Wang**[2]

[1] Department of Electrophysics, National Chiao Tung University, Hsinchu, Taiwan, Republic of China
[2] Institute of Electro-Optics, National Chiao Tung University, Hsinchu, Taiwan, Republic of China

Received: 7 June 1999/Revised version: 3 August 1999/Published online: 30 November 1999

Abstract. An analytical model is developed to study the influence of the Auger upconversion process on the thermal loading under lasing and nonlasing conditions. With the developed model, Auger upconversion rates can be determined by comparing theoretical calculations with experimental results for the ratio of the thermal loading under lasing and nonlasing conditions. The upconversion rates obtained with the present method are compared with the results measured from the fluorescence decay experiment.

PACS: 42.55.Rz

Diode-pumped solid-state lasers have been shown to be efficient, compact, and reliable all-solid-state optical sources. Neodymium-doped laser crystals are widely used in diode-pumped solid-state lasers. The thermal effect is the main factor in scaling diode-end-pumped Nd-doped crystal lasers to high power [1]. Recently, a number of papers [2–6] show that the upconversion process has a significant influence on the population mechanisms of the Nd-doped laser crystals at high excitation densities, leading to much larger thermal loading. The high excitation densities are typically found under nonlasing conditions, Q-switched operation, or operation as an amplifier. Therefore, knowledge of the Auger upconversion rate is important for designing a laser system with high excitation densities. The fluorescence decay measurement is often used to determine the upconversion rate in laser materials. Guyot et al. [7] performed the fluorescence decay experiment and reported that the values of the upconversion rate in Nd:YLF and Nd:YAG are $(1.7 \pm 1) \times 10^{-16}$ cm^3/s and $(2.8 \pm 1) \times 10^{-16}$ cm^3/s, respectively. Ostroumov et al. [8] used the same method and reported that the upconversion rates in Nd:LSB and Nd:GVO_4 are $(2–6) \times 10^{-16}$ cm^3/s and $(1–1.4) \times 10^{-15}$ cm^3/s, respectively.

In scaling end-pumped lasers to higher power, the fiber-coupled laser-diodes with circular beam profiles are often used as pump sources because the high-power diode lasers are very asymmetric in their emitting aperture dimensions. In this work, we developed an analytical model to consider the influence of Auger upconversion on the thermal loading in fiber-coupled diode-end-pumped lasers under lasing and nonlasing conditions. With the derived formulae, the values of upconversion rates can be determined from the best fit of theoretical calculations to experimental results for the thermal loading without and with laser action. The present model provides a method to estimate the Auger upconversion rates. The practical examples of Nd:YAG and Nd:YVO_4 crystals are considered to illustrate the utility of the present model.

*Corresponding author.
Present address: Department of Electrophysics, National Chiao Tung University, 1001 TA Hsueh Road, Hsinchu 30050 Taiwan (Fax: +886-35/729-134, E-mail: yfchen@cc.nctu.edu.tw)

1 Theoretical modeling

The Auger upconversion process involves two nearby ions in the metastable $^4F_{3/2}$. One ion returns to the $^4I_{9/2}$, $^4I_{11/2}$ or $^4I_{13/2}$ level by transferring its energy to the other ion that is, in turn, brought into a higher excited state. To take Auger upconversion effects into account, the rate equation for inversion population density before laser action is given by [9]:

$$\frac{\mathrm{d}n}{\mathrm{d}t} = R(r,z) - \frac{n}{\tau} - \gamma n^2 \,, \tag{1}$$

where n is the population density, $R(r,z)$ is the rate of the pump intensity at any radial location r or axial location z, τ is the emission lifetime, and γ is the upconversion rate. Here we neglect the self-quenching effect, i.e. the cross relaxation, which could be significant at a high dopant concentration [4]. Since the crystals studied here were 1.0% Nd:YAG and 0.5% Nd:YVO_4 crystals, the cross relaxation is negligible. Under cw excitation, the population density of the laser level is obtained by setting $\mathrm{d}n/\mathrm{d}t = 0$; therefore,

$$n(r,z) = \left[\sqrt{1 + 4\tau^2\gamma R(r,z)} - 1\right] / 2\tau\gamma \,. \tag{2}$$

Using a fiber-coupled laser diode in an end-pumping configuration, the pump rate can be expressed as a top-hat

distribution:

$$R(r,z)=\frac{P_{\rm in}}{h\nu_{\rm p}}\frac{\alpha {\rm e}^{-\alpha z}}{\pi\omega_{\rm p}^2\left[1-{\rm e}^{-\alpha l}\right]}\Theta(\omega_{\rm p}^2-r^2)\ , \tag{3}$$

where $P_{\rm in}$ is the incident pump power, $\nu_{\rm p}$ is the pump frequency, α is the absorption coefficient at the pump wavelength, $\omega_{\rm p}$ is the pump size, l is the length of the active medium, and $\Theta()$ is the Heaviside step function.

The total population number is found by integrating the population density over the crystal volume

$$N=\int_0^l {\rm d}z\int_0^{\omega_{\rm p}} n(r,z)2\pi r{\rm d}r\ . \tag{4}$$

It can be found that if $\gamma=0$, the average population number is given by $N_{\rm o}=\tau P_{\rm in}/h\nu_{\rm p}$. Therefore, the fractional reduction of the population inversion due to upconversion can be expressed as

$$F_{\rm uc}=(N_{\rm o}-N)/N_{\rm o}\ . \tag{5}$$

Substituting (2)–(4) into (5), and integrating over the medium length and transverse dimensions, the fractional reduction can be found to be

$$F_{\rm uc}(N_{\rm o})=1-\frac{2}{\varrho(1-{\rm e}^{-\alpha l})}\left\{2\left(\sqrt{1+\varrho}-\sqrt{1+\varrho{\rm e}^{-\alpha l}}\right)+\ln\left[\frac{{\rm e}^{-\alpha l}\left(2+\varrho-2\sqrt{1+\varrho}\right)}{2+\varrho{\rm e}^{-\alpha l}-2\sqrt{1+\varrho{\rm e}^{-\alpha l}}}\right]-\alpha l\right\}\ ,$$

where

$$\varrho=\frac{4\gamma\tau\alpha}{\pi\omega_{\rm p}^2}N_{\rm o}\ . \tag{6}$$

With $\gamma=0$, i.e. no upconversion effects, one can find $F_{\rm uc}(N_{\rm o})=0$.

Figure 1 shows the dependence of $F_{\rm uc}(N_{\rm o})$ on the average population number $N_{\rm o}$ by using various different Auger upconversion rates and the parameters of the 0.5 at. % Nd:YVO_4 system in our experiment: $\omega_{\rm p}=400\,\mu$m, $l=7$ mm, $\alpha=10\,{\rm cm}^{-1}$ and $\tau=100\,\mu$s. It can be seen that the reduction factor $F_{\rm uc}(N_{\rm o})$ is an increasing function of the average population number $N_{\rm o}$. Even though the average population number $N_{\rm o}$ below threshold is proportional to the incident pump power $P_{\rm in}$, for a cw laser above threshold, the inversion density is clamped to the critical inversion at the threshold condition. As a consequence, the reduction factor for a cw laser above threshold should be determined by $F_{\rm uc}(N_{\rm th})$, where $N_{\rm th}=\tau P_{\rm th}/h\nu_{\rm p}$ and $P_{\rm th}$ is the threshold pump power.

The excited ion involving in the Auger process relaxes down to the $^4F_{3/2}$ level mostly via multiphonon emission. Accordingly, the Auger upconversion process reduces the inversion population density and increases the thermal loading in laser materials. Neglecting the contribution from the cross-relaxation process, the total thermal loading in laser materials can be given by [10]

$$P_{\rm load}=P_{\rm qd}+P_{\rm uc}, \tag{7}$$

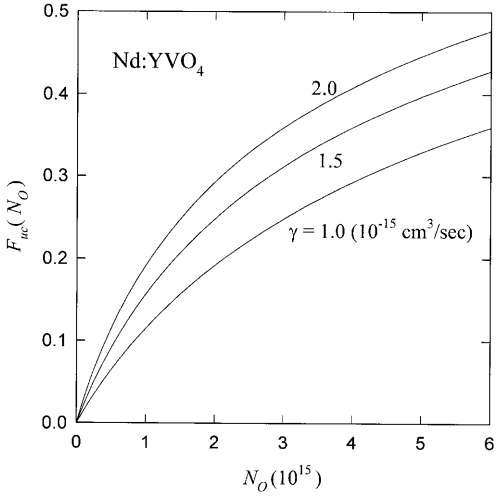

Fig. 1. Dependence of $F_{\rm uc}(N_{\rm o})$ on the average population number $N_{\rm o}$ with $\omega_{\rm p}=400\,\mu$m, $l=7$ mm, $\alpha=10\,{\rm cm}^{-1}$ and $\tau=100\,\mu$s

where $P_{\rm qd}$ is the thermal power deposited by the quantum defect and $P_{\rm uc}$ is the thermal loading caused by the upconversion. Under lasing conditions, the heat from the quantum defect is determined from the difference between the pump photon energy and the lasing photon energy. On the other hand, under nonlasing conditions, the heat from the quantum defect depends upon the difference between the pump photon energy and the fluorescence photon energy. Therefore, the thermal loading caused by the quantum defect is given by [10]

$$P_{\rm qd}=\begin{cases}\left[\left(\lambda_{\rm l}-\lambda_{\rm p}\right)/\lambda_{\rm l}\right]P_{\rm in} & \text{for lasing condition}\\ \left[\left(\lambda_{\rm f}-\lambda_{\rm p}\right)/\lambda_{\rm f}\right]P_{\rm in} & \text{for nonlasing condition}\end{cases}\ , \tag{8}$$

where $\lambda_{\rm l}$ is the laser wavelength, $\lambda_{\rm p}$ is the pump wavelength, and the average fluorescence wavelength $\lambda_{\rm f}$ is given by $\int\lambda f(\lambda){\rm d}\lambda/\int f(\lambda){\rm d}\lambda$, where $f(\lambda)$ is the relative fluorescence spectrum. To calculate the average fluorescence wavelength, fluorescence spectra were measured with an optical spectrum analyzer (Advantest Q8347) which enhanced the performance of spectrum analyzer (0.01-nm resolution) employing a Fourier spectrum system with a Michelson interferometer. Figure 2 shows the fluorescence spectrum of the 0.5% Nd:YVO_4 pumped by a 808-nm fiber-coupled laser diode in the region of 900–1400 nm. With the fluorescence spectra, $\lambda_{\rm f}$ was found to be 1032 nm and 1038 nm for Nd:YVO_4 and Nd:YAG, respectively.

From the definition of the factor $F_{\rm uc}$, the number of ions involving in the Auger process for the nonlasing condition can be expressed as $F_{\rm uc}(N_{\rm o})(P_{\rm in}/h\nu_{\rm p})$. On the other hand, the number of ions involving in the Auger process for the lasing condition is given by $F_{\rm uc}(N_{\rm th})(P_{\rm th}/h\nu_{\rm p})$ because the inversion density is clamped to the critical inversion at the threshold condition. From the known Stark-level splitting [11], the possible upconversion processes in Nd:YVO_4 crystal consist of the transitions $^4F_{3/2}\rightarrow{}^4D_{3/2}$, $^4F_{3/2}\rightarrow{}^4G_{9/2}+{}^4G_{11/2}+{}^2K_{15/2}$, and $^4F_{3/2}\rightarrow{}^4G_{7/2}$ which result from the downconversion transitions $^4F_{3/2}\rightarrow{}^4I_{9/2}$, $^4F_{3/2}\rightarrow{}^4I_{11/2}$, and $^4F_{3/2}\rightarrow{}^4I_{13/2}$, respectively. In Nd:YAG the possible upconversion processes include $^4F_{3/2}\rightarrow{}^2K_{15/2}+{}^2D_{3/2}$, $^4F_{3/2}\rightarrow{}^4G_{9/2}+{}^4G_{11/2}$, and $^4F_{3/2}\rightarrow{}^4G_{7/2}+{}^2K_{13/2}+{}^2G_{7/2}$, which arise from the downconversion transitions $^4F_{3/2}\rightarrow{}^4I_{9/2}$,

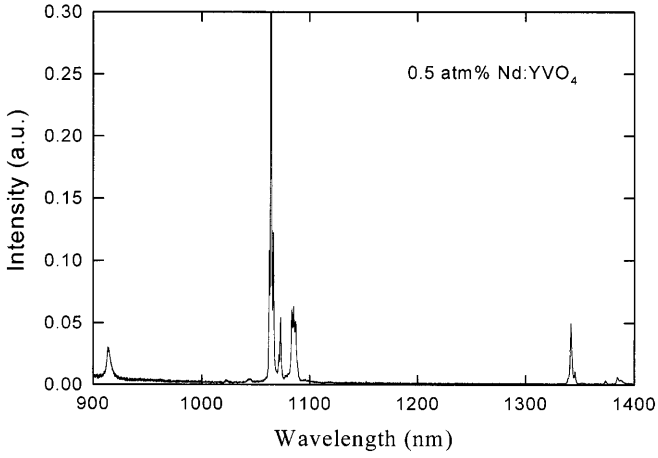

Fig. 2. Fluorescence spectrum of the 0.5 at. % Nd:YVO_4 in the region of 900–1400 nm

$^4F_{3/2} \rightarrow {}^4I_{11/2}$, and $^4F_{3/2} \rightarrow {}^4I_{13/2}$, respectively. The heat generated from the upconversion processes is due to the multiphonon relaxation from the excited level back to the upper laser level. Therefore, the energy of the multiphonon relaxation is equal to the energy of the correlated downconversion transitions. Since it is rather difficult to estimate the relative contribution of each upconversion channel for nonlasing conditions, we assume that the probability of the upconversion processes is proportional to the fluorescence spectrum. In terms of the average fluorescence wavelength, the contribution of the downconverted ion of an upconversion process to the thermal load can be given by

$$P_{\mathrm{uc}} = \begin{cases} F_{\mathrm{uc}}\left(N_{\mathrm{o}}\right)\left(P_{\mathrm{in}}/h\nu_{\mathrm{p}}\right)h\nu_{\mathrm{f}} = \left(\lambda_{\mathrm{p}}/\lambda_{\mathrm{f}}\right)F_{\mathrm{uc}}\left(N_{\mathrm{o}}\right)P_{\mathrm{in}} \\ \qquad\qquad \text{for nonlasing conditions} \\ F_{\mathrm{uc}}\left(N_{\mathrm{th}}\right)\left(P_{\mathrm{th}}/h\nu_{\mathrm{p}}\right)h\nu_{\mathrm{f}} = \left(\lambda_{\mathrm{p}}/\lambda_{\mathrm{f}}\right)F_{\mathrm{uc}}\left(N_{\mathrm{th}}\right)P_{\mathrm{th}} \\ \qquad\qquad \text{for lasing conditions} \end{cases} . \tag{9}$$

With (7)–(9), the total thermal loading can be analytically expressed as

$$P_{\mathrm{load}} = \begin{cases} \left[1-\left(\lambda_{\mathrm{p}}/\lambda_{\mathrm{f}}\right)\right]P_{\mathrm{in}} + \left(\lambda_{\mathrm{p}}/\lambda_{\mathrm{f}}\right)F_{\mathrm{uc}}\left(N_{\mathrm{o}}\right)P_{\mathrm{in}} \\ \qquad\qquad \text{for nonlasing conditions} \\ \left[1-\left(\lambda_{\mathrm{p}}/\lambda_{\mathrm{l}}\right)\right]P_{\mathrm{in}} + \left(\lambda_{\mathrm{p}}/\lambda_{\mathrm{f}}\right)F_{\mathrm{uc}}\left(N_{\mathrm{th}}\right)P_{\mathrm{th}} \\ \qquad\qquad \text{for lasing conditions} \end{cases} . \tag{10}$$

Then the ratio of the thermal loading without and with laser action can be given by

$$P = \begin{cases} 1 & \text{below threshold} \\ \dfrac{\left[1-\left(\lambda_{\mathrm{p}}/\lambda_{\mathrm{f}}\right)\right]P_{\mathrm{in}} + \left(\lambda_{\mathrm{p}}/\lambda_{\mathrm{f}}\right)F_{\mathrm{uc}}\left(N_{\mathrm{o}}\right)P_{\mathrm{in}}}{\left[1-\left(\lambda_{\mathrm{p}}/\lambda_{\mathrm{l}}\right)\right]P_{\mathrm{in}} + \left(\lambda_{\mathrm{p}}/\lambda_{\mathrm{f}}\right)F_{\mathrm{uc}}\left(N_{\mathrm{th}}\right)P_{\mathrm{th}}} & \text{above threshold} \end{cases} . \tag{11}$$

2 Determination of upconversion rate

With the present model, we have considered the upconversion-induced heat generation in Nd:YVO_4 and Nd:YAG crystals end-pumped by a fiber-coupled laser diode under both lasing and nonlasing conditions. The laser wavelength for lasing conditions was 1064 nm for both Nd:YVO_4 and Nd:YAG crystals. The laser crystals were wrapped with indium foil and were press-fitted into a copper housing with cylindrical symmetry. A thermocouple was embedded in the copper housing and near to the edge of the laser crystal. The periphery of the copper housing was held at $T_0 = 293$ K. Under edge-cooled conditions [12], the end faces of the laser crystal and the copper housing are virtually insulating in comparison to the heat transfer across the radial surface. Based on this approximation, the steady-state temperature distributions in the laser crystal and copper housing are given by the solution of the linear heat diffusion equation. Therefore, the heat flow through the laser crystal is equal to the heat flow through the copper housing and is proportional to $K(T_1 - T_0)$, where T_1 is the temperature of the embedded thermocouple and K is the thermal conductivity of the copper housing. In other words, the ratios of the thermal loading in laser crystals without and with laser action can be determined from the ratios of the $(T_1 - T_0)$ under nonlasing and lasing conditions. Strictly speaking, the thermal conductivity is not a constant but depends upon temperature. For pure copper, the thermal conductivity varies from 387 $\mathrm{W\,m^{-1}K^{-1}}$ at 273 K to 379 $\mathrm{W\,m^{-1}K^{-1}}$ at 373 K. To avoid a significant deviation from the temperature dependence of the thermal conductivity, the thermal resistance of the copper housing was designed to lead to the maximum $(T_1 - T_0)$ in all experiments below 50 K.

The experimental results for 0.5% Nd:YVO_4 are compared in Fig. 3 to the theoretical results (solid lines) calculated from (1) and (11) by using the parameters used in Fig. 1. Experimental results show that the thermal loading at 10-W pump power increases by a factor of ≈ 2.0 times owing to the upconversion process. The value of the upconversion rate deduced from Fig. 3 is about $(1.5 \pm 0.5) \times 10^{-15}$ $\mathrm{cm^3/s}$. Since Nd:YVO_4 crystal is similar to Nd:GVO_4 crystal, we made a comparison between these two crystals. It can be found that the obtained upconversion rate in Nd:YVO_4 crystal is close to the value in Nd:GVO_4 crystal, $(1–1.4) \times 10^{-15}$ $\mathrm{cm^3/s}$, obtained by Ostroumov et al. from the fluorescence decay measurement [8]. To our knowledge, this is the first time the upconversion rate in Nd:YVO_4 has been estimated. Figure 3 also shows that the upconversion macroparameter γ is not a universal characteristic of the given laser crystal at different pump powers. Generally, the energy transfer mechanism consists of static and migration-assisted processes. As shown in [8], the description of upconversion in terms of γn^2 is not applicable in the case of static upconversion and is also limited in the case of migration-assisted upconversion in the diffusion regime. If the upconversion parameter γ is deduced from the experiments that cannot be precisely fitted in terms of γn^2, different values of γ can be obtained, depending on many experimental factors and other material parameters. This is one of the most probable reasons why there is a systematic deviation between the experimental data points and the calculated curve. Even though the present experimental results cannot be completely explained with the model by using a simple term γn^2 in the rate equation, we can use it to estimate the effective value of γ.

Figure 4 shows the experimental data and theoretical calculations for the ratios of the thermal loading in 1.0% Nd:YAG crystal without and with laser action. The theor-

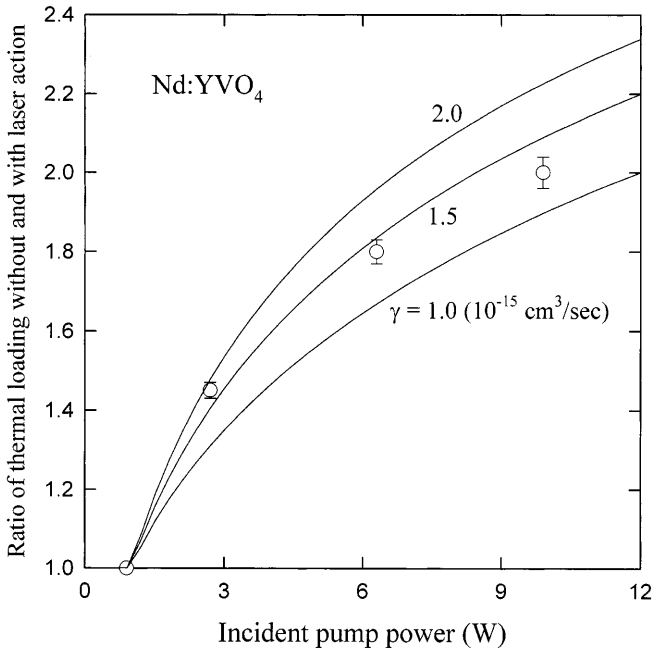

Fig. 3. Ratios of the thermal loading in Nd:YVO_4 crystal without and with laser action: experimental results (*symbol*) and theoretical calculations (*solid lines*)

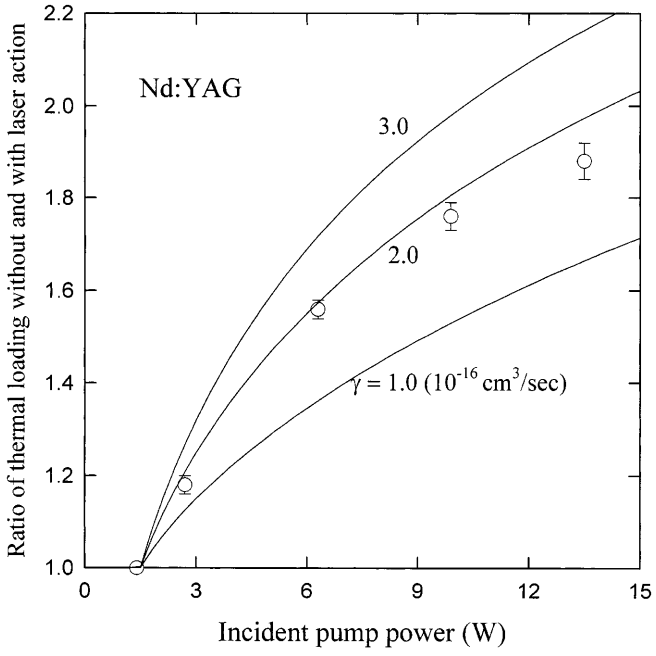

Fig. 4. Ratios of the thermal loading in Nd:YAG crystal without and with laser action: experimental results (*symbol*) and theoretical calculations (*solid lines*)

etical results are calculated by using the following parameters: $\omega_p = 400\,\mu m$, $l = 10\,mm$, $\alpha = 8\,cm^{-1}$ and $\tau = 230\,\mu s$. The value of the upconversion rate deduced from Fig. 4 is about $(1.8 \pm 0.2) \times 10^{-16}\,cm^3/s$. This result is between the value $(2.8 \pm 1) \times 10^{-16}\,cm^3/s$ reported by Guyot et al. [7] and the value $0.5 \times 10^{-16}\,cm^3/s$ deduced from the data of Guy et al. [4]. The reason why there is a deviation between the present result and other works may be due to the deficiency of the model with a simple term γn^2, as discussed in the Nd:YVO_4 result.

Finally, it is worthwhile to mention that the present formulae are similar to those in the recent article by Hardman et al. [13] and that article appeared after the present work was performed. Even so, Hardman et al. investigate Nd:YLF crystal whereas the present work focuses on the estimation of upconversion parameters for Nd:YAG and Nd:YVO_4 crystal. In addition, we use the temperature rise to determine the ratios of thermal loading instead of using the thermal lens parameter.

3 Conclusions

A theoretical model has been developed to consider the influence of Auger upconversion on the thermal loading under lasing and nonlasing conditions. With this model, upconversion rates can be determined from the best fit of theoretical calculations to experimental results. The practical examples of Nd:YAG and Nd:YVO_4 crystals are performed to illustrate the utility of the present model. We believe that the present model can be applied to other Nd-doped laser materials and used to minimize the negative influence of upconversion in laser design.

References

1. C. Pfistner, R. Weber, H.P. Weber, S. Merazzi, R. Gruber: IEEE J. Quantum Electron. **QE-30**, 1605 (1994)
2. M. Pollnau, W.A. Clarkson, D.C. Hanna: Conference on Lasers and Electro-Optics, CLEO '98 OSA Technical Digest Series **6**, 100 (1998)
3. J.L. Blows, T. Omatsu, J. Dawes, H. Pask, M. Tateda: IEEE Photonics Technol. Lett. **10**, 1727 (1998)
4. S. Guy, C.L. Bonner, D.P. Shepherd, D.C. Hanna, A.C. Tropper, B. Ferrand: IEEE J. Quantum Electron. **QE-34**, 900 (1998)
5. T. Chuang, R. Verdún: IEEE J. Quantum Electron. **QE-32**, 79 (1996)
6. M. Pollnau, P.J. Hardman, W.A. Clarkson, D.C. Hanna: Opt. Commun. **147**, 203 (1998)
7. Y. Guyot, H. Manaa, J.Y. Rivoire, R. Moncorgé, N. Garnier, E. Descroix, M. Bon, P. Laporte: Phys. Rev. B **51**, 784 (1995)
8. V. Ostroumov, T. Jensen, J.P. Meyn, G. Huber, M.A. Noginov: J. Opt. Soc. Am. B **15**, 1052 (1998)
9. S.A. Payne, L.K. Smith, R.J. Beach, B.H.T. Chai, J.H. Tassano, L.D. DeLoach, W.L. Kway, R.W. Solarz, W.F. Krupke: Appl. Opt. **33**, 5526 (1994)
10. F. Balembois, F. Falcoz, F. Kerboull, F. Druon, P. Georges, A. Brun: IEEE J. Quantum Electron. **QE-33**, 269 (1997)
11. A.A. Kaminskii: *Laser crystals*, 2nd edn. (Springer, Berlin, Heidelberg, 1990) pp. 129–130
12. A.K. Cousins: IEEE J. Quantum Electron. **QE-28**, 1057 (1992)
13. P.J. Hardman, W.A. Clarkson, G.J. Friel, M. Pollnau, D.C. Hanna: IEEE J. Quantum Electron. **QE-35**, 647 (1999)